Check for updates

Application of Multiphase Interleaving Parallel Technology in Oilfield Energy Storage Power Supply

Chao He(✉), Tao Jiang, and Wang Qu

Beijing Institute of Precision Mechatronics and Controls, Beijing 100076, China
hechaohit@163.com

Abstract. In order to cope with harsh environment and vibration, oil field energy storage requires high reliability and maintainability, high consistency in the use of power devices, and redundancy in battery charging and discharging. In this paper, an energy storage power supply is designed. The front and rear parts use the same three-phase bridge circuit, the front part is rectifier/inverter circuit, and the rear part is buck/boost circuit for charging and discharging. The grid side parameters are designed, The rear part uses three-phase parallel to improve redundancy, and uses the interleaved parallel method to meet the grid side parameters used in the battery side charge and discharge circuit, so that the front and rear parts can be interchanged and universal, easy to maintain, and reduce the volume of inductance and capacitance. The problem of current sharing is solved and the control loop is designed. Through simulation and field application, good results are obtained.

Keywords: Energy storage · Interleaving parallel connection · Current sharing

1 Introduction

The problem: the drilling crew of Oilfield works and lives in the field all the year round, and each drilling crew has several containers to form a working and living place. Living and office power is provided by a 68 kW diesel generator. When the generator is under light load, the efficiency is low and the noise is high, so it is not suitable to operate continuously for 24 h. A quiet and efficient power supply is required.

Solution: an energy storage power supply with power battery and automatic switching of charge and discharge can provide a quiet and efficient power supply for the living and office power of the field drilling crew. The energy storage power supply is composed of a set of power lithium batteries with a total of 25 kWh, a power module and a bypass module. Power battery provides storage of electric energy; The power module completes the functions of rectification, inversion, charge and discharge; The bypass module is the power switch interface, including electricity detector, change-over switch, bypass switch, main circuit break, capacitor bank and operation screen.

The energy storage power supply is designed as the front part and the rear part. The front part is AC/DC and the rear part is DC/DC; For simplifying the design, the front

L. Yan and J. Na (Eds.): ICFPMCE 2022, AHE 10, pp. 214–234, 2023.
https://doi.org/10.2991/978-94-6463-022-0_19

part and rear part are designed as a mirror structure, that is, a three-phase bridge circuit structure composed of the same devices is used. The front part is three-phase AC/DC, which makes rational use of three-phase bridge circuit; The rear part is a DC/DC circuit, which can make three phases in parallel to form a phase. The charging circuit is a buck circuit composed of the antiparallel diode of the upper IGBT(Insulated Gate Bipolar Transistor) and the lower IGBT. The discharging circuit is boost circuit composed of the antiparallel diodes of the lower IGBT and the upper IGBT. The rear part uses 1/3 phase-shifting PWM interleaving parallel, which can save inductance and greatly reduce volume and cost.

With the concept of carbon neutralization gaining popularity, energy storage technology has been widely concerned and applied [1, 2]. In this paper, the oil field energy storage power supply is designed, and the energy storage technology is applied to the oil field power supply. The interleaved parallel technology is used in the energy storage power supply of oil field, the volume of the energy storage power supply in the oil field is greatly increased and the applicability is increased. This paper describes the design process of interleaving parallel technology and realizes multiphase interleaved parallel connection; And the current sharing technology in interleaving parallel is designed. Literature [4–6] introduces bi-directional converters applied in different fields in interleaved parallel and literature [9–15] mentions a new interleaved parallel, but it cannot be well used in the symmetrical circuit of oil field energy storage. The current sharing method described in literature [7, 8] needs communication and is closed-loop, so it is difficult to correct parameters. The direct modulation ratio average current sharing method designed in this paper is simple and reliable, especially suitable for interleaving parallel current sharing. The energy storage power supply described in literature [3] does not use staggered parallel connection and has a large volume.

In this paper, the three-phase interleaved parallel technology is used to realize the bidirectional conversion of energy storage in the symmetrical circuit of energy storage bidirectional converter, so that the circuit structure of network side and charging side is consistent and interchangeable (Fig. 1).

Two kinds of CPUs are widely used in energy storage converter. One is DSP2000 series of TI company and the other is STM32 series of ST company. A timer is used for each phase of PWM generation in DSP. For interleaved parallel connection, it is only necessary to add 1/3 cycle to the counter corresponding to each phase timer during initialization. However, STM32 uses an advanced timer to control a three-phase bridge. There is only one timer, so it is impossible to use carrier phase-shifting interleaving in parallel. This must be achieved using three timers, each of which controls a bridge arm.

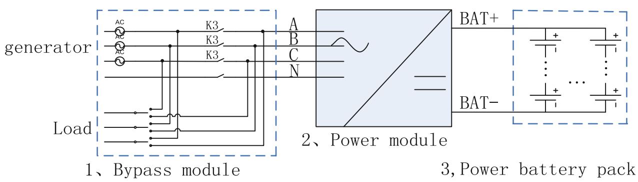

Fig. 1. Schematic diagram of energy storage power supply for oil field

2 Working Principle

The energy storage power supply can be charged and discharged automatically. After startup, it operates automatically without manual intervention.

When the diesel generator is turned on, the system detects an incoming power of electricity and enters into charging;

When the diesel generator is switched off, the system detects that there is no power of electricity and enters into discharge;

When charging, the diesel generator is turned off, the system detects that there is no power, turns off, and then discharges will start up;

When discharging, the diesel generator is turned on, the system detects an incoming power, turns off, and then charges will start up;

The power module is composed of front part and rear part. The front part is AC/DC, which is composed of an IPM, three-phase inductance and three-phase AC filter capacitor. The rear part is DC/DC, which is also composed of an IPM, three-phase inductance and three-phase DC filter capacitor. In the middle is a DC bus with large capacity DC support capacitor.

During charging, the electric energy goes from the generator to the power battery. When the change-over switch is closed, the power of the generator enters the power module. The front part is an AC/DC rectifier. The latter part is a DC/DC buck charger, which charges the power battery according to the set current; At the same time, the generator is supplied to the load through the bypass switch of the bypass module.

When discharging, the electric energy flows from the power battery to the load. The change-over switch is open. The latter part is a DC/DC booster; The front part works in the inverter state which invert three-phase AC supply load.

The interleaved parallel structure plays a key role in the system when it is used in the later part circuit. It makes it possible for the front and rear parts to use the same circuit structure.

3 Main Circuit Structure

3.1 Main Circuit

The main circuit includes front part bidirectional AC/DC, rear part bidirectional DC/DC.

The main circuit structure is shown in Fig. 2. The front part is bidirectional AC/DC, which is composed of a three-phase inverter circuit composed of IPM, a three-phase LC filter circuit and a main circuit breaker. In charging mode, ABC connects the generator through change-over switch, and the electric energy is from left to right. The front part is a rectifier circuit, which rectifies the AC into 540 V DC to the intermediate DC bus; In discharging mode, ABC is connected to the AC user load through change-over switch, and the electric energy is from left to right. The front part is an inverter circuit, which reverses the intermediate DC voltage into three-phase 380 V AC for the user. The rear part is bidirectional DC/DC, with the same structure as the front part. The rear part is a buck circuit, which reduces the electric power of the intermediate DC bus to the battery voltage for charging. In discharging mode, the electric energy is from right to left. The

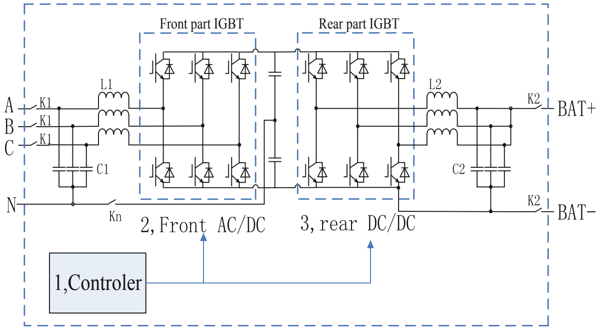

Fig. 2. Main circuit of energy storage power supply

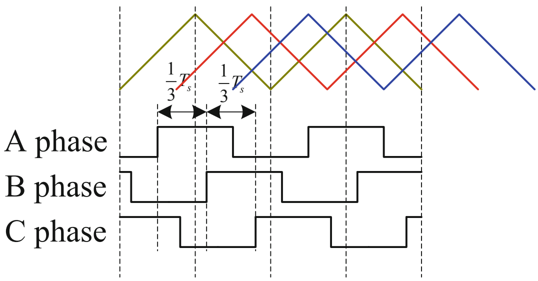

Fig. 3. Interleaved parallel carrier phase shifting

rear part is a boost circuit, which raises and the battery power to 600 V for the front part inverter.

The interleaved parallel circuit is in the later part of the main circuit. The later part IPM is a three-phase bridge circuit. Each phase (bridge arm) is an independent buck/boost circuit. When the software sends PWM to each phase, the interleaved parallel is realized by carrier phase shifting. As shown in Fig. 3.

Interleaved parallel structure: the three-phase bridge of rear part is connected to the LC filter circuit which is composed of L2 and C2, and then the output of the filter circuit is connected to a point in front of K2, which is the circuit structure to realize parallel connection. In software control mode, the software sends the same PWM to three-phase bridge, and the three phases are connected in parallel to form one phase. In each carrier, the PWM is shifted 1/3 carrier period, and then the interleaved parallel is realized. The Fig. 3 is the Interleaving parallel waveform when the duty cycle is 50%. The waveform of phase B lags behind that of phase A by 1/3 carrier period, i.e. 1/3 switching cycles; Phase C lags behind phase B by 1/3 switching cycle. The upper part of Fig. 3 is the triangular wave for PWM wave generation. The software sets the output of PWM module to the triangular wave waveform with lag of 1/3 per phase as shown in the Fig. 3. The output can generate the Interleaved PWM waveform as shown in Fig. 3 to drive the IGBT.

The controller is composed of CPU and peripheral functional circuits. As shown in the Fig. 4, the CPU is stm32f407, and the periphery is sampling circuit, IO circuit, PWM driving circuit and communication circuit. The sampling circuit samples the generator

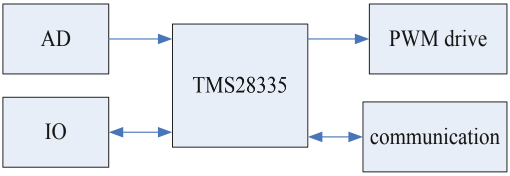

Fig. 4. Schematic diagram of controller

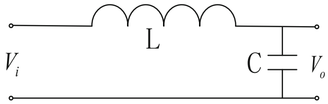

Fig. 5. LC filter circuit

terminal voltage, input AC current, DC voltage, inverter output AC voltage, output AC current and temperature; The IO circuit drives all switches of the system; The PWM driving circuit amplifies the PWM signal to drive the IGBT of the main circuit inverter; Communication circuit connects the operation screen, i.e. HMI module.

3.2 Main Circuit Design and Calculation

1. DC voltage value design
   For the rear part circuit, in charging mode, the rear part regulates, the front part does not regulate, and the three-phase bridge is directly used as the uncontrollable rectifier circuit. Considering the fluctuation range of AC input, the DC voltage value is 380ac $\pm$ 10% $\times$ 1.414 = 537 $\pm$ 10% = 483.3 ~ 590.7 V. In discharging mode, the system outputs as inverter, DC voltage required: $>$380 + 10% = 590.7 V. To sum up, the DC voltage is set at 600 V.
2. Switching frequency
   Switching frequency is related to heat dissipation and system volume and IGBT working frequency. The switching frequency of IGBT is less than 20 kHz. In order to save the volume of radiator, the switching frequency of energy storage power supply is set as 10 kHz.
3. Filter LC calculation
   The output inductor and AC capacitor form an output filter, whose main purpose is to filter out the frequency near the switching frequency. As shown in Fig. 5.

The transfer function G(s) of LC filter is:

$$G(s) = \frac{V_o(s)}{V_i(s)} = \frac{\frac{1}{LC}}{s^2 + \frac{1}{RC}s + \frac{1}{LC}} = \frac{\omega_n^2}{s^2 + 2\zeta\omega_n S + \omega_n^2} \tag{1}$$

where, $\omega_n = \frac{1}{2\pi\sqrt{LC}}$ is the corner frequency of the transfer function. It is related to the parameters of inductance (L) and capacitance(C). In order to filter out harmonics near the switching frequency, the corner frequency shall be less than 1/5 of the switching frequency f_s, i.e.:

$$\frac{1}{2\pi\sqrt{LC}} \le \frac{1}{5}f_s \tag{2}$$

In addition, the maximum pulsating current on L($\Delta I_{L\max}$):

$$\Delta I_{L\max} = \frac{V_s - V_o}{\sqrt{3}}\frac{1}{2Lf_s} \tag{3}$$

V_o is the output DC voltage, V_s is the power supply voltage.

Generally, the maximum pulsating current on L shall less than 20% of the peak current I_N, that is:

$$\frac{U_{dc} - E_s}{\sqrt{3}}\frac{1}{2Lf_s} \le 20\%\sqrt{2}I_N \tag{4}$$

The value of L can be calculated from Eq. (5):

$$L \ge \frac{U_{dc} - E_s}{\sqrt{3}}\frac{1}{2f_s}\frac{1}{20\%\sqrt{2}I_N} \tag{5}$$

DC voltage: $U_{dc} = 610$ V, AC voltage: $E_s = 380 * 1.414$, switching frequency: $f_s = 10000$ Hz, Rated current: $I_N = 15$ A. Calculated: L = 427 uH, selected: L = 600 uH.

The value of C can be calculated from Eq. (6):

$$C \ge \frac{5^2}{4\pi^2 L f_s^2} \tag{6}$$

Calculated: C = 10.55 uF, selected: C = 10 uF.

4 Current Sharing Design

Three phase work in parallel must require consideration of current imbalance. Each phase will cause current imbalance due to different device parameters and distribution parameters. Interleaving makes IGBT opening inconsistent, which is also the factor leading to current imbalance.

4.1 Current Sharing Method

The current sharing method includes the average current method: the three-phase output current is sampled in real time, calculate the average. The sampling circuit of each phase calculates a difference with the average. The difference directly compensates the PI output and changes the PWM directly. Of course, the loop uses one PI, that is, the feedback current is the sum of the three-phase currents:

Another method is PI regulation method: each phase current uses one PI regulator. This method is only applicable to current loop or current loop existed. Control is complex.

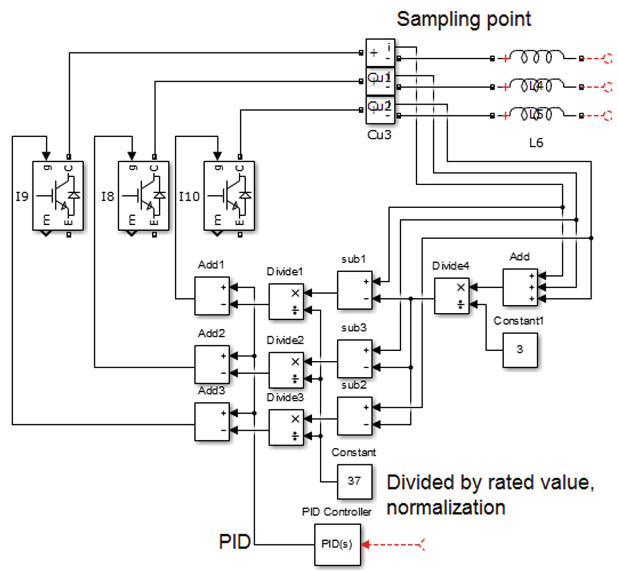

Fig. 6. Current sharing method

This system adopts one PI and adopts the average current method (Fig. 6). i_A, i_B, i_C is the sample value of three-phase current, i_{AVG} is the average current.

$$i_{AVG} = \frac{1}{3} \times (i_A + i_B + i_C) \tag{7}$$

$$i_{A\_f} = i_A - i_{AVG} \tag{8}$$

The voltage control equation can be obtained:

$$u'_{PI} = u_{PI} - i_{A\_f}/i_{AN} \tag{9}$$

u'_{PI} is the PI control value after current sharing; u_{PI} is the PI control value, a normalized value, and the value range is $[-1\ 1]$; i_{AN} is the maximum current of phase A, that is, the phase current value when the duty cycle is 1, that is, i_{A_f}/i_{AN} is the normalized value exceeding the average current, and u_{PI} subtracting it to obtain the PI control value after current sharing u'_{PI}. The current sharing value is directly subtracted from the PWM control value to achieve the current sharing effect. Since the current-sharing value is the current value, this method is more suitable for the current loop control.

This process is completely digital, especially suitable for digital control.

4.2 Sampling Time Point

Notice, the waveform of the inductor current is as follows:

It can be seen that the waveform of the inductor current is a DC current superimposed triangular wave. During a switching cycle, the current first rises and then falls.

$$\frac{di}{dt} = \frac{u}{L} \tag{10}$$

The rate of rise and fall of the inductor current is inversely proportional to the inductance value and proportional to the voltage. In the interleaved parallel system, in order to reduce the volume, the inductance is relatively small, so the current slope is higher, but the current sampling value will have a large difference in different sampling time point. If the sampling of phase A is fixed in one position, then phase A will be sampled at the same position every sampling cycle, which is not a big problem, but the sampling of phase B and C is also sampled at this position, then the three-phase current will have a big difference, and the higher the load, the greater the difference. Appropriate sampling points must be set for phases B and C.

The first method: use three identical ADs, all started with their own PWM. For example triple ADC mode of the STM32F407.

The second method: Set the appropriate AD conversion time, which is the same as the time of the carrier phase shift, and the sampling time of the three currents is exactly the time of the phase shift.

This system adopts the first method, which uses triple AD, which is set to start AD in respective PWM.

5 Equivalent Inductance Calculation

The most important function of the interleaved parallel is to reduce the inductor value and the inductor volume. To calculate the inductance, the first step is to use the continuous current inductance formula to calculate the minimum inductance that makes the inductor current continuous. On the other hand, the value of the inductance is determined from the current ripple analysis.

According to the calculation formula of BUCK circuit inductance:

$$L = \frac{V_o}{2rI_o} DT_s \tag{11}$$

D is the duty cycle and T_s is the switching cycle. (usually current coefficient r = 0.4), and then input the parameters of this system.

$K_{rising} = \frac{V_s - V_o}{L}$ is the rising slope of the inductor current, the falling slope of the inductor: $K_{falling} = -\frac{V_o}{L}$

.

Taking the case of critical continuity of single-phase inductive current as an example, The conclusion is also applicable to the case of continuous inductive current. As shown in Fig. 7, the blue line is the synthesis of three-phase inductive current, and the ripple is greatly reduced. Add a coordinate system to Fig. 8, and mark points such as A, B, C,

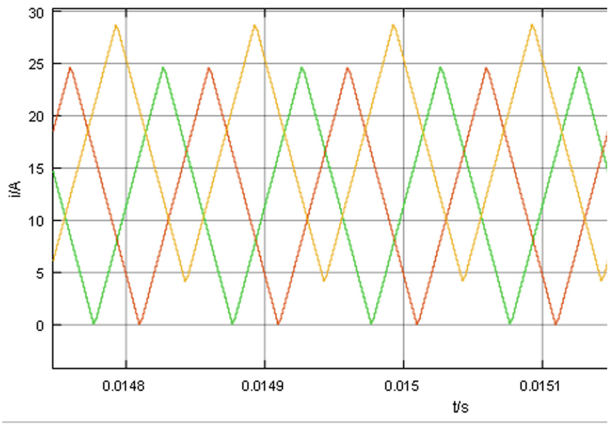

Fig. 7. Inductor current waveform

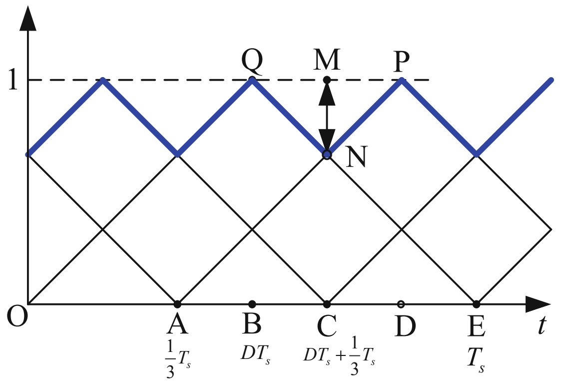

Fig. 8. Schematic diagram of inductive current at critical continuity

D, E, Q, M, N and P in the figure, MN is the current ripple after interleaving in parallel, and the ripple in single-phase is BQ.

The horizontal axis is time, OE is a switching cycle T_s, the time of point A is $\frac{1}{3}T_s$ and the time of point C is $DT_s + \frac{1}{3}T_s$.

The vertical axis is current. According to the rise rate of the inductive current, it can be concluded that the current value at point Q is $\frac{V_s - V_o}{L}DT_s$, and so the current value at point M is $\frac{V_s - V_o}{L}DT_s$ too.

Then write the expression of QE line segment and AP line segment with two-point formula, calculate the intersection N, and then calculate the length of MN to obtain the ripple after interleaving and combining.

5.1 Analysis of Inductance Current Ripple in Parallel Only

When the inductive current is critical continuous and continuous, the inductive current ripple when only parallel connection without interleaving is QB:

$$\Delta I_{L(parallel)} = \frac{V_o}{L}(1-D)T_s = \frac{V_s}{L}D(1-D)T_s \tag{12}$$

When the three phases are connected in parallel, the ripple of the inductance current is added because it is in the same phase. Then the three inductors are equivalent to parallel connection.

Calculate the output voltage ripple:

$$\begin{aligned}\Delta u_c &= \frac{1}{C}\int_{t1}^{t2} idt \\ &= \frac{1}{C} \times \frac{I_{\max} - I_{\min}}{2} \times (t2 - t1) \times \frac{1}{2} = \frac{1}{8}\frac{\Delta I_L}{C}T_s\end{aligned} \tag{13}$$

Among them, ΔI_L is the ripple of the inductance current. It can be seen that a large inductance current will cause a large ripple of the output voltage.

5.2 Inductance Current in Interleaved Parallel Connection

According to the falling slope of inductive current $K_{falling} = -\frac{V_o}{L}$ and point E (T_s, 0), the expression of line QE is obtained:

$$i_{t1(falling)}(t) = -\frac{V_o}{L}t + \frac{V_o}{L}T_s \tag{14}$$

According to According to the rising slope of inductance current $K_{rising} = \frac{V_s - V_o}{L}$ and point A($\frac{1}{3}T_s$, 0), the expression of line AP is obtained:

$$i_{t2(rising)}(t) = \frac{V_s - V_o}{L}t + \frac{V_s - V_o}{L}\frac{T_s}{3} \tag{15}$$

Let $i_{t1(falling)}(t) = i_{t2(rising)}(t)$, get the time at N: $t = \frac{1}{3}(2D+1)T_s$.

Substituting into Eq. (14), we can get:

$$i_N = \frac{V_o}{L}(\frac{2(1-D)}{3})T_s \tag{16}$$

The current at M:

$$i_M = \frac{V_s - V_o}{L}DT_s = \frac{V_o(1-D)}{L}DT_s \tag{17}$$

Then the inductance current ripple after interleaving:

$$\Delta I_{L(interleaving)} = i_M - i_N = \frac{V_s}{L}D(\frac{1}{3}(1-D))T_s \tag{18}$$

Compare with Eq. (12) to obtain the ripple ratio:

$$\Delta I_{L(interleaving)}/\Delta I_{L(parallel)} = \frac{1}{3} \tag{19}$$

In other words, the ripple current of inductance after interleaving is 1/3 of that of direct parallel, which is a universal conclusion.

5.3 Check the Inductance Value and Ripple

1. Calculation of inductance value in direct parallel connection:

$$L = \frac{270}{2 \times 0.4 \times 12.3} 0.5 \times 0.0001 = 0.0014H \tag{20}$$

   It has exceeded the design inductance at the grid side of 600 uH.

2. Calculation of inductance value in interleaved parallel connection: $L = \frac{270}{2 \times 0.4 \times 12.3} 0.5 \times 0.0001/3 = 457\,\mu\text{H}$ It is just 600 uH less than the design inductance at the grid side. Conditions are met.

6 Control Loop Design

The front part is controlled by rectifier and inverter, using traditional methods. The control loop of the rear part is mainly designed here.

6.1 Charging BUCK Current Loop

In charging mode, the rear part is a buck circuit, because charging is the current charging object, and the control loop is designed as a single loop current loop (Fig. 9).

$K_p + \frac{K_I}{s}$ is the PI equivalent model.

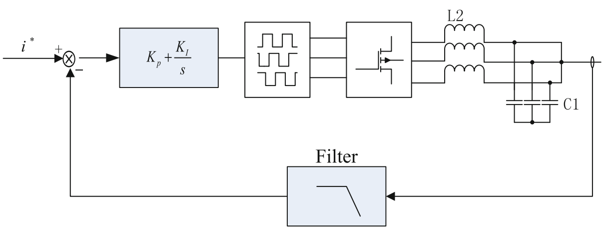

Fig. 9. Charging buck current loop

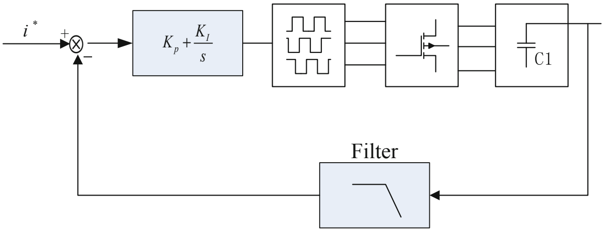

Fig. 10. Discharge BOOST voltage loop

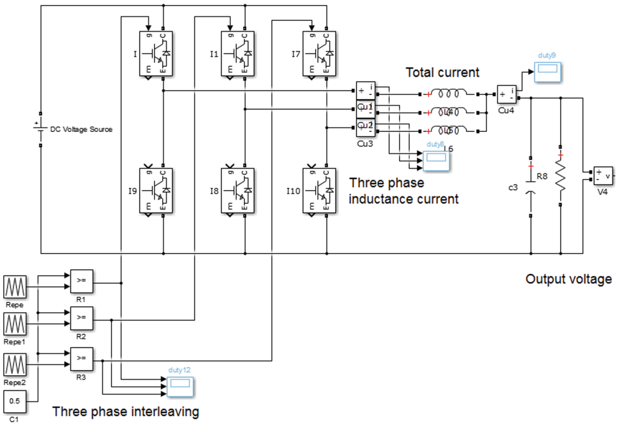

Fig. 11. Charging buck parallel simulation circuit

6.2 Discharge BOOST Voltage Loop

In discharging mode, the rear part is a boost circuit, the control target is the intermediate DC voltage, and the control loop is designed as a single loop voltage loop (Fig. 10).

7 Simulation and Run Effect

According to the designed system structure and parameters, simulation verification is carried out. The feasibility of interleaved parallel is verified and compared with the method of direct parallel, i.e. no interleaved.

7.1 Simulation of Interleaved Parallel Charging Buck

First of all, simulation operation of charging mode when direct parallel in for the rear part, which is the buck circuit at this time. In order to verify the function, use open-loop simulation method, inputs 540 V DC voltage and outputs 270 V battery voltage, so the duty cycle is 50%. The simulation circuit is as in Fig. 11.

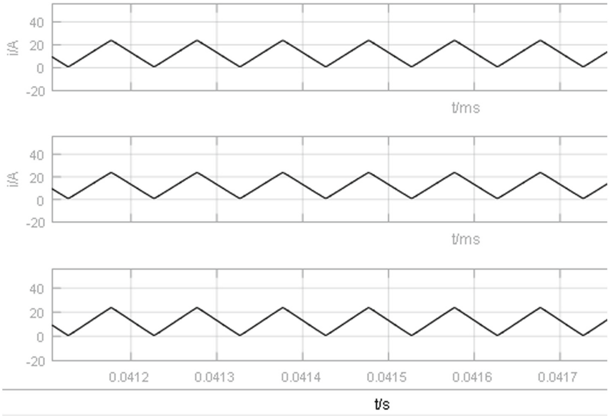

Fig. 12. Current waveform of direct parallel three-phase inductance

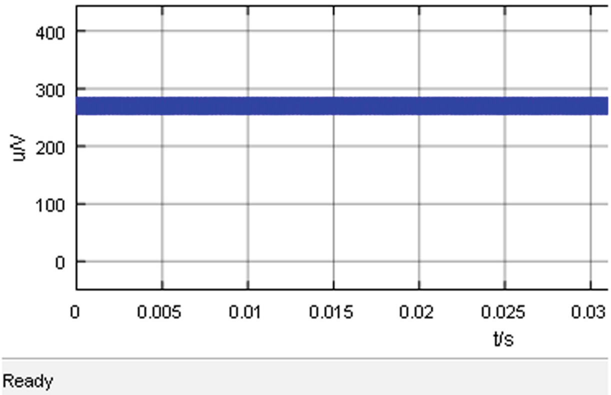

Fig. 13. Direct parallel output voltage waveform

The simulation results are shown in Fig. 12 and Fig. 13. The three-phase inductance current is a triangular wave in the same phase, which is consistent with the theoretical derivation.

It can be seen from Fig. 13 that the inductance current has a large ripple, the ripple reaches 25 A, and the total output current is 12.5 A in one phase. The peak value of ripple current reaches 2 times of the total output current because the inductance at the AC side is small in one phase. It can be seen from Fig. 14 that the output voltage fluctuates greatly, reaching as much as 30 V, accounting for 11% of the rated output voltage of 270 V, which seriously exceeds the standard. This is also because the inductance and capacitance at the AC side are too small and the filtering effect is poor.

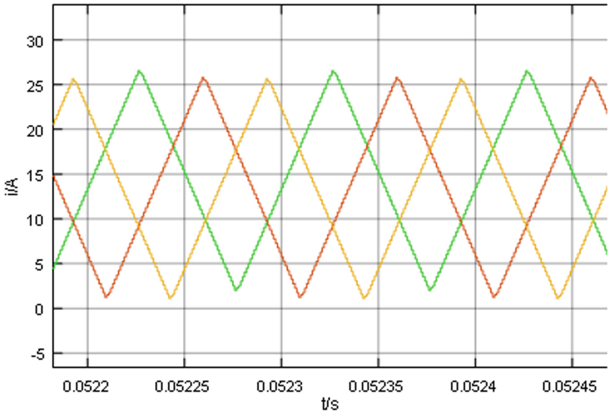

Fig. 14. Inductance current waveform of interleaved three-phase

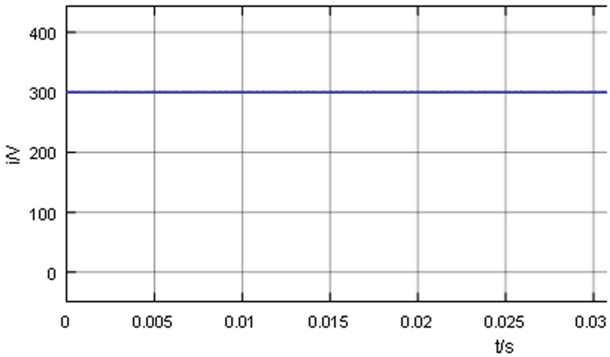

Fig. 15. Output voltage waveform of interleaved three-phase

The second step is to simulate the same circuit with interleaved parallel connection. Only the generated triangular waves are interleaved in parallel. Operation results are shown in Fig. 15 and Fig. 16.

It can be seen from Fig. 15 that the inductance current of each phase still fluctuates greatly, reaching 25 A, which is the same as that of non interleaved. This is also because the inductance of each phase is small, because the circuit structure and circuit parameters of each phase have not changed. However, it can be seen from Fig. 16 that the output voltage has been greatly improved. Note that since the output load is a pure resistance, the output current is also the same as that in Fig. 16. The fluctuation is very small, and only <2 v is read from the figure, which fully conforms to the index. This is the effect of interleaved complementarity. The specific process is fully described in Sect. 5.

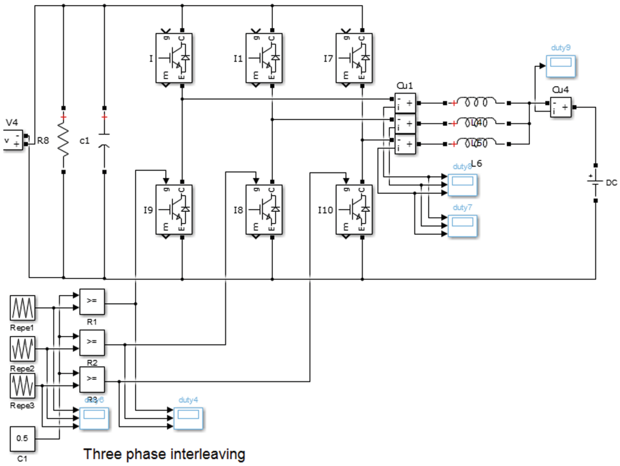

Fig. 16. Discharge BOOST parallel simulation circuit

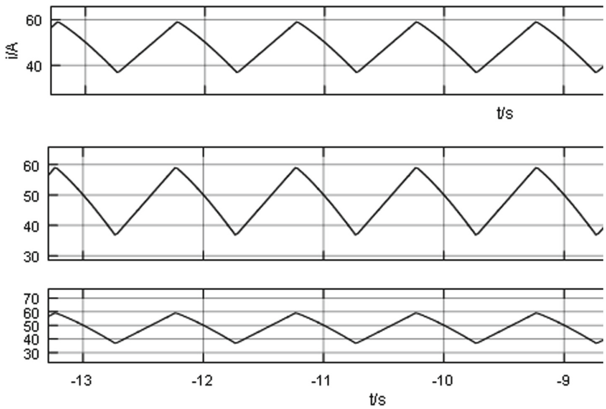

Fig. 17. Boost direct parallel three-phase inductance current waveform

7.2 Simulation of Interleaved Parallel Connection of Discharge BOOST

First, the simulation operation of non interleaved parallel connection in discharge mode is carried out for the rear part. At this time, the rear part is BOOST circuit. To verify the function, use open-loop simulation, the input is 270 V of the battery in rightmost, and the output is DC voltage. The target is 600 V, so the duty cycle is set to: d = 1 − Vi/Vo = 55%. The simulation circuit is as in Figs. 16, 17, 18, 19 and 20.

From Fig. 18, 19, and 20, it can be seen that the situation is similar to that of BUCK, and the inductance current fluctuation is the same, but after interleaving, the output voltage fluctuation is very small, meeting the design index.

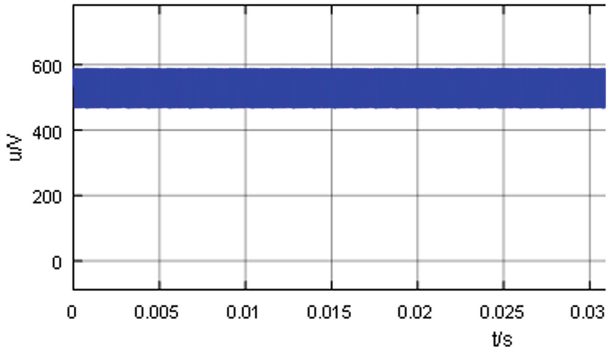

Fig. 18. Boost direct parallel output voltage waveform

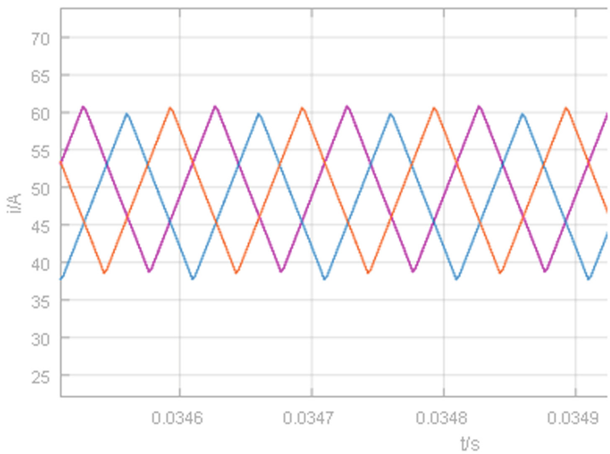

Fig. 19. Boost interleaved three-phase inductance current waveform

7.3 Interleaved Parallel Current Sharing Simulation

On the basis of Fig. 11, the equivalent series resistance value on the inductance is modified, and the three phases are set to 0.01, 0.008 and 0.001 respectively. The simulation results show that the following waveforms are obtained. The inductance current is obviously unbalanced, and the unbalance degree reaches 25%.

According to the current sharing method shown in Fig. 21, the following inductance current waveforms are obtained through simulation under 20% load and 100% load (Figs. 22 and 23).

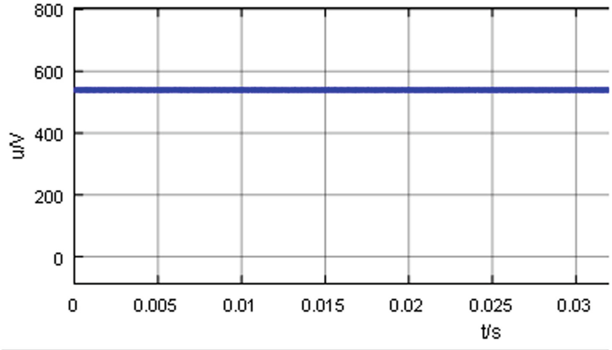

Fig. 20. Boost interleaved three-phase output voltage waveform

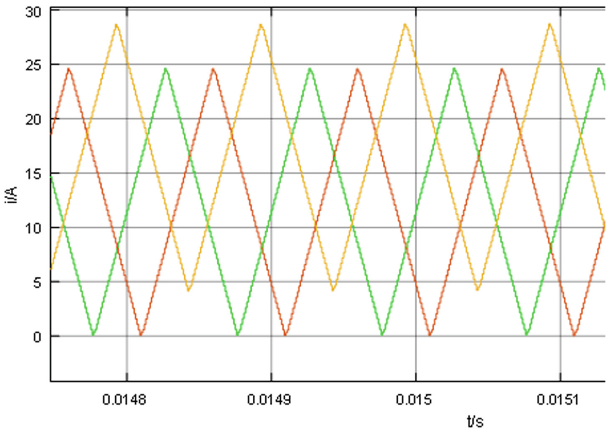

Fig. 21. Three phase inductance current unbalance

It can be seen that the current consistency is particularly good after current sharing. Through the current sharing algorithm, the current consistency is less than 1% at 20% load and less than 0.5% at 100% load. The current sharing effect is very good.

7.4 Field Deployment of Energy Storage Power Supply

The energy storage power supply based on interleaved parallel technology has been applied in oil field and deployed in multiple drilling crews (Fig. 24).

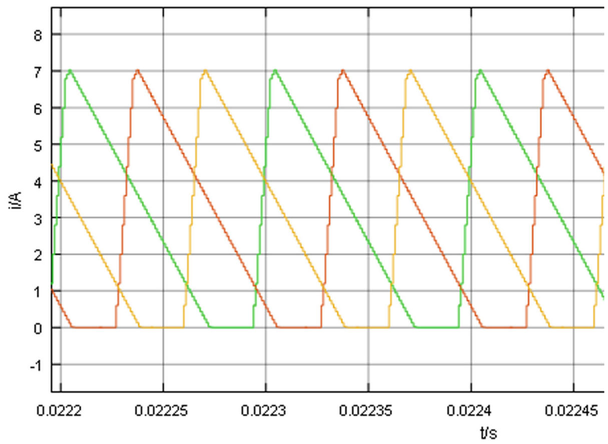

Fig. 22. Three phase inductance current in 20% load current sharing

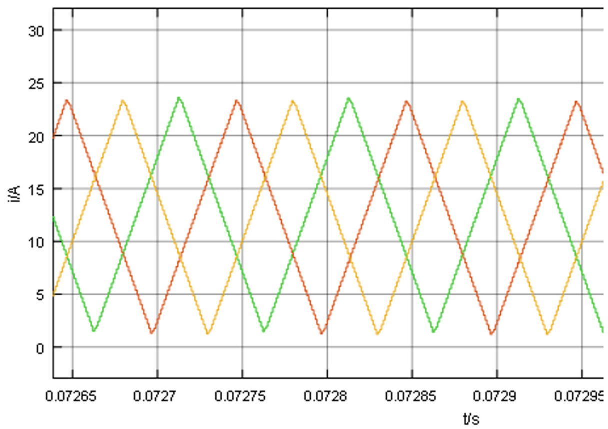

Fig. 23. Three phase inductance current after 100% load current sharing

The generator and the energy storage power supply are installed side by side. The generator is connected to the energy storage power supply through 380 V power cable. The energy storage power supply leads a 380 V power cable to the user's container house to supply power to the house.

Figure 25 is the internal diagram of the energy storage power supply module. In the box is the power module with 10kW configuration. The upper and lower boards are the same. On the board are all the power units: switches, inductors and capacitors. Two boards can be used in common.

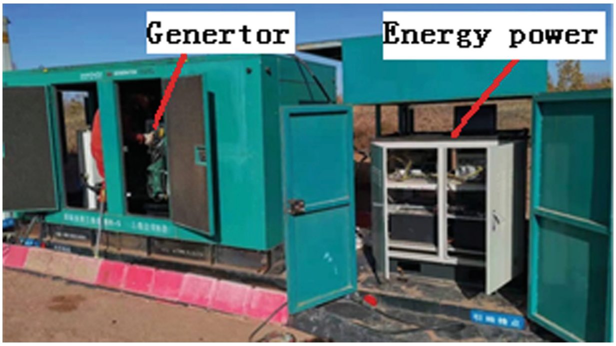

Fig. 24. Figure of energy storage power supplies

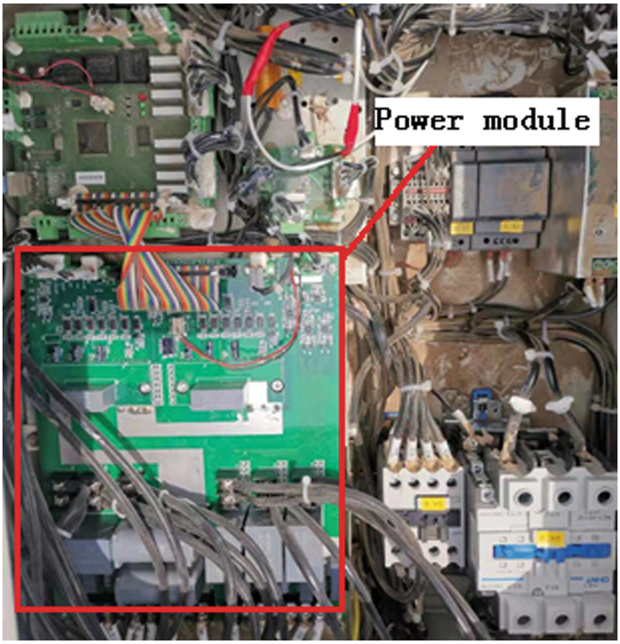

Fig. 25. Power module

8 Conclusion

It is suitable for oil field energy storage, and is designed into a consistent interchangeable circuit between the grid side and the battery side. The battery side uses the interleaved parallel algorithm, which makes the charging circuit meet the index requirements and solves the current sharing problem. PI parameters are designed by using current loop charge and discharge to achieve good response and charging efficiency. Through simulation and practical application, good operation results are obtained.

Acknowledgments. Thank my tutor, Professor Zhang Donglai, for his guidance and help over the years, and thank the members of our team for their hard work and unremitting efforts.

Authors' Contributions. Hechao (1980-), male, communication author, master, engineer, His main research interests include power electronic control technology, high-power power supply control technology, high step-down ratio converter and high-power drive; E-mail: hechaohit@163.com.

Jiang Tao (1985-), male, master, engineer, mainly engaged in high-power power electronic AC conversion.

Wang Qu (1985-), male, master, engineer, mainly engaged in high-power drive.

References

1. Liu, Y., Liu, C., Wang, W., et al.: Analysis of development status and trend of energy storage technology. SINO_GLOBAL ENERGY, **22**(4), 80–88 (2017). (in Chinese)
2. Jiang, H., Du, E., Zhu, G., et al.: Review and prospect of seasonal energy storage for power system with high proportion of renewable energy. Autom. Electr. Power Syst. **44**(19), 194–207 (2020). (in Chinese)
3. Xu, H., Shao, Y., Su, X., et al.: The application of large-power interleaved technology in power supply of the tram. Power Electron. **52**(2), 7–9 (2018)
4. Lv, F., Li, Z.: Analysis and application of staggered parallel technology in ripple suppression for the bidirectional DC converter. Instrum. Technol. **1**(10), 5–9 (2017)
5. Li, C., Zhang, B., Han, X., et al.: Circulating current suppression method for paralleled bi-directional power converters based on adaptive virtual damping control. High Volt. Eng. **46**(5), 1550–1559 (2020)
6. Lu, Z., Zhu, W., Liu, J., et al.: A novel interleaved parallel bidirectional DC/DC converter. Proc. CSEE **32**(12), 39–46 (2013)
7. Zhang, J., Xie, X., Wu, X., et al.: Research on active current-sharing methods for DC/DC converters. Proc. CSEE **25**(19), 31–36 (2005)
8. Zhao, L., Wu, Y., Chen, Z., et al.: Study on current sharing strategy about series capacitor interleaved boost converter in full-duty range **40**(7), 2330–2338 (2020)
9. Li, X., Huang, J., Wang, D., et al.: Photovoltaic charging control system for electric tricycles with staggered parallel technology. Proc. CSEE **36**(11), 2909–2917 (2016). (in Chinese)
10. Wang, J.B., Kao, D.: Impedance interference investigation of the paralleled DC/DC converters system used droop current sharing control. In: 2015 IEEE 2nd International Future Energy Electronics Conference, Taipei, China, pp. 1–5. IEEE (2015)
11. Li, Y., Wang, M., Liang, H., Wang, S.: Study on distribution controlled inverter parallel system with different power ratings. Power Syst. Prot. Control **42**(6), 123–128 (2014)
12. Antoszczuk, P.D., Retegui, R.G., Funes, M., et al.: Interleaved current control for multiphase converters with high dynamics mean current tracking. IEEE Trans. Power Electron. **31**(12), 8422–8434 (2016)
13. Quan, Z., Li, Y.: Impact of PWM schemes on the common-mode voltage of interleaved three-phase two-level voltage source converters. IEEE Trans. Industr. Electron. **66**(2), 852–864 (2019)
14. Qiu, D., Zhang, B., Wei, C.: Study of paralleled buck converters with improved automatic current-sharing technique. Trans. China Electrotech. Soc. **20**(10), 45–51 (2005)
15. Antoszczuk, P., Retegui, R.G., Uicich, G.: Interleaved boundary conduction mode versus continuos conduction mode magnetic volume comparison in power converters. IEEE Trans. Power Electron. **31**(12), 8037–8041 (2016)